Local density pseudopotential calculations for molecules: O2 and Mo2O2S2(S2)2− 2

J. Bernholc and N. A. W. Holzwarth

Citation: The Journal of Chemical Physics **81**, 3987 (1984); doi: 10.1063/1.448139
View online: http://dx.doi.org/10.1063/1.448139
View Table of Contents: http://scitation.aip.org/content/aip/journal/jcp/81/9?ver=pdfcov
Published by the AIP Publishing

Local density pseudopotential calculations for molecules: O_2 and $Mo_2O_2S_2(S_2)_2^{2-}$

J. Bernholc and N. A. W. Holzwarth[a)]
Exxon Research and Engineering Company, Corporate Research Science Laboratories, Annandale, New Jersey 08801

(Received 4 November 1983; accepted 27 June 1984)

We report a development of a self-consistent, local density pseudopotential method for calculation of the electronic properties of large molecules. Angular momentum dependent, first-principles ionic pseudopotentials are used to describe the valence-core interactions. Average correlation effects are included in the local density sense. The wave functions, the charge density and the exchange-correlation potential are expanded in atom-centered Gaussian orbitals of *s*, *p*, and *d* symmetry. These atomic basis sets account for nonspherical (non-muffin tin) effects and are easily transferable to different geometries and other environments. The total energy of the system is accurately evaluated. The method is tested on the O_2 molecule and found to give the orbital energies, the equilibrium distance and the vibrational frequency in good agreement with previous all-electron calculations. As the first application to a large system, we have investigated the electronic structure of the $Mo_2O_2S_2(S_2)_2^{2-}$ anion. In this anion, the molybdenum atoms are fivefold coordinated: to one oxygen atom, two bridging sulfur atoms, and a molecular S_2. From the energy level diagram, the oxygen atoms are found to form approximately triple bonds to the molybdenum atoms, the Mo–S and Mo–S_2 bonds being successively weaker. The molybdenum atoms form a single Mo–Mo bond and are formally in the Mo(V) oxidation state. The highest occupied molecular orbitals are, however, the S_2 π^* orbitals, oriented perpendicular to the Mo-S_2 planes and located almost 1 eV above the Mo–Mo bond energy. The lowest unoccupied molecular orbitals are the relatively closely spaced π^* antibonding Mo–O, Mo–Mo, and Mo–S_2 orbitals.

I. INTRODUCTION

Understanding of bonding and reactive properties of molecules often calls for accurate electronic structure calculations of relatively large systems. We describe development of a method combining several recent advances in both solid state physics and quantum chemistry. The resulting method is efficient, while at the same time sufficiently accurate to give a good description of bonding and dissociation properties. Even very complex bonding patterns are accurately explained such as those of antiferromagnetically coupled, multiply bonded Mo_2 and Cr_2 (Ref. 1). In this paper we give a detailed account of the method, test it on the O_2 molecule, and apply it to the newly synthesized $Mo_2O_2S_2(S_2)_2^{2-}$ molecule.

The major problem in a first-principles method is an accurate description of the effects of electronic correlation. These effects are usually described by either configuration interaction treatment or by electron-gas parametrization. The latter one is considerably simpler and was adopted for the present work. The earliest and simplest is the X_α parametrization, developed by Slater,[2] the electron-gas exchange contribution to the total energy is adjusted to reproduce the exact Hartree–Fock energy of an atom.[3] In the later local density formalism,[4] the exchange and correlation contributions are both extracted from electron-gas calculations.[5] The local density correlations are approximate, but they include contributions from an infinite number of configurations. Local density treatments are thus advantageous when the important configurations are not known at the outset or when their number is large as found in the transition metal systems.[1]

The use of pseudopotentials has led to great advances in solid state physics. In this work, we demonstrate the applicability of local density pseudopotentials to molecular systems.

In a pseudopotential approach, the core electrons are assumed frozen, while the core-valence interactions are simulated by an effective potential. The resulting pseudo-wave functions are nodeless and only valence electrons enter the calculations explicitly. Heavy atom molecules can thus be treated as easily as the first row ones. The local density pseudopotentials are generated from atomic calculations without any empirical adjustments.[6,7] The relativistic effects are also included.[8]

The calculations were carried out using the method of Gaussian expansions.[9] In this method the orbitals are expanded in Gaussians; the charge density and the exchange-correlation potentials are each fitted to auxiliary sets of Gaussian functions. In contrast to the multiple-scattering X_α method,[10] the nonspherical effects are included in the calculations. Furthermore, the total energy of the system can be accurately calculated, allowing for optimization of geometries.

The O_2 molecule has been studied by several methods.[11–17] For this reason, we have chosen to study this molecule as a test of the present method. Our results are in excellent agreement with previous all-electron calculations.

The newly synthesized $Mo_2O_2S_2(S_2)_2^{2-}$ (Ref. 18) molecule is a representative member of the large class of compounds which serve as synthetic models of molybdoenzyme active sites[19(a)] and of the active sites in hydrodesulfurization (HDS) and hydrodenitrogenation (HDN) catalysis.[19(b)] We

[a)] Present address: Department of Physics, Wake Forest University, Winston–Salem, North Carolina 27109.

 0021-9606/84/213987-09$02.10

have carried out a detailed analysis of bonding in this molecule in terms of Mulliken populations, contour maps, and frontier orbitals.

This paper is organized as follows: A short summary of local density theory is given in Sec. II; the pseudopotential formalism and the calculations are described in Secs. III and IV, respectively. In Sec. V the method is tested on the O_2 molecule; and in Sec. VI the application to the $Mo_2O_2S_2(S_2)_2^{2-}$ system is reported. Section VII contains a summary of the paper.

II. LOCAL DENSITY THEORY

In local density theory one self-consistently solves the equations[4] (in Rydbergs)

$$-\nabla^2\psi_i + \left[\int \frac{2\rho(\mathbf{r}')}{|\mathbf{r}-\mathbf{r}'|}\,d\mathbf{r}' + \sum_{j=1}^{M} V_j(\mathbf{r}-\mathbf{R}_j) + \mu_{\rm xc}^{\sigma}(\rho,\zeta)\right]\psi_i = \epsilon_i\psi_i, \quad (1)$$

$i = 1,...,N,$

where N is the number of electrons in the system, ψ_i and ϵ_i are the one-electron wave functions and eigenvalues, respectively, M is the number of nuclei, and V_j is the nuclear potential at the position R_j. The many-body electronic interactions are represented through the exchange-correlation potential $\mu_{\rm xc}^{\sigma}$, where σ denotes the spin direction of the orbital ψ_i. This potential depends only on the total charge density

$$\rho(\mathbf{r}) = \sum_{i=1}^{N} |\psi_i(\mathbf{r})|^2 \quad (2)$$

and the spin density

$$\zeta(r) = [\rho^{+}(\mathbf{r}) - \rho^{-}(\mathbf{r})]/\rho(\mathbf{r}). \quad (3)$$

For cases where $\rho^{+}(r) = \rho^{-}(r)$ or where the spin dependence in Eq. (1) is neglected, the orbitals are identical for both spin-up and spin-down electrons.

Even in the spin dependent case, the ψ_i can be readily interpreted in the molecular orbital picture, making analysis as easy as in the simplest parametrized methods.

One should note in particular that the total potential in Eq. (1) is orbital independent. This is not the case in configuration interaction methods.

Equation (1) is derived rigorously[4] from the expression for the total energy of the system

$$E_{\rm tot} = T + V_{\rm ee} + E_{\rm xc} + V_{\rm en} + V_{\rm nn}, \quad (4)$$

where T is the kinetic energy, $V_{\rm ee}$ is the classical electron–electron interaction, $E_{\rm xc}$ is the exchange-correlation contribution to the total energy, and $V_{\rm en}$ and $V_{\rm nn}$ are the electron–nucleus and nucleus–nucleus electrostatic interaction energies. The explicit expressions for these terms are

$$T = \sum_{i=1}^{N} \int \psi_i^{*}(-\nabla^2)\psi_i\,d\mathbf{r}, \quad (5)$$

$$V_{\rm ee} = \frac{1}{2}\int\int \frac{2\rho(\mathbf{r})\rho(\mathbf{r}')}{|\mathbf{r}-\mathbf{r}'|}\,d\mathbf{r}\,d\mathbf{r}', \quad (6)$$

$$E_{\rm xc} = \sum_{\sigma}\int \epsilon_{\rm xc}^{\sigma}(\rho,\zeta)\rho^{\sigma}(\mathbf{r})d\mathbf{r}, \quad (7)$$

$$V_{en} = \int \rho(\mathbf{r})\sum_j V_j(\mathbf{r}-\mathbf{R}_j)d\mathbf{r}, \quad (8)$$

and

$$V_{nn} = \frac{1}{2}\sum_{\substack{j,j'\\ j\neq j'}} \frac{2Z_jZ_{j'}}{|R_j - R_{j'}|}, \quad (9)$$

where $\epsilon_{\rm xc}^{\sigma}$ is the exchange-correlation energy density and Z_j are the nuclear charges.

By multiplying Eq. (1) by $\psi_i(r)$, integrating over $\mathbf{r}$ and summing over the occupied orbitals one obtains

$$E_{\rm tot} = \sum_{i}^{\rm occ}\epsilon_i - \frac{1}{2}\int\int \frac{2\rho\rho'}{|\mathbf{r}-\mathbf{r}'|}\,d\mathbf{r}\,d\mathbf{r}' + \sum_{\sigma}\int [\epsilon_{\rm xc}^{\sigma}(\rho,\zeta) - \mu_{\rm xc}^{\sigma}(\rho,\zeta)]\,\rho^{\sigma}(\mathbf{r})d\mathbf{r} + V_{\rm nn}, \quad (10)$$

where the second term corrects for the double counting of the electron–electron interaction in the sum over one-electron eigenvalues.

From the several parametrizations of $\epsilon_{\rm xc}^{\sigma}$ and $\mu_{\rm xc}^{\sigma}$ available in the literature,[20–23] we have chosen the parametrization of Vosko *et al.*,[22] which is fitted to the accurate electron-gas of Ceperley and Alder[24] and has a new, more accurate description of the spin polarization energy.

III. PSEUDOPOTENTIAL FORMALISM

The modern ionic pseudopotentials[6,7] which describe the core-valence interactions are constructed from atomic all-electron calculations. The resulting pseudopotentials $V_{\rm ps}$ and pseudo-wave functions ϕ_i with eigenvalues ϵ_i satisfy the atomic Schrödinger equation

$$-\nabla^2\phi_i + \left[V_{\rm ps} + \int \frac{2\rho'_{\rm ps}}{|\mathbf{r}-\mathbf{r}'|}\,d\mathbf{r}' + \mu_{\rm xc}^{\sigma}(\rho,\zeta)\right]\phi_i = \epsilon_i\phi_i, \quad (11)$$

$i = 1,...,n_v,$

where $\rho_{\rm ps}$ and n_v denote the pseudocharge density and the total number of valence electrons, respectively. The pseudopotentials, pseudo-wave functions, and their derivatives match exactly the real valence potentials and wave functions beyond a matching radius, typically much smaller than half the bond length. The pseudo-wave functions are nodeless and reproduce exactly the valence eigenvalues. Equation (11) is self-consistent in the pseudocharge density.

As a result of the above constraints, the pseudopotentials are angular momentum dependent. Their effect on the pseudo-wave function ϕ is

$$V_{\rm ps}\phi = \sum_l V_{{\rm ps},l}(r)P_l\phi, \quad (12)$$

where P_l projects the appropriate l component from the pseudo-wave function ϕ.

We should mention here, that the effective core potentials, first introduced by Goddard and co-workers[25] and commonly used in Hartree–Fock and GVB calculations are also angular momentum dependent and of the form (12). These ECP, originally defined with help of matrix elements over a given basis set[25] and later refined[26] to allow for a fully numerical generation of the ECP, are not suitable for local density calculations.

The nonlinearity of the exchange-correlation potential requires, for greatest accuracy, the use of the full charge density in the evaluation of μ_{xc}^{σ} (Ref. 27). The dependence of μ_{xc}^{σ} on the total charge density ρ can be simplified without significant loss of accuracy by noting that the nonlinearity of μ_{xc}^{σ} is important only when ρ_{ps} and the core charge density ρ_c are of comparable magnitude. Thus, instead of ρ_c, one can use $\tilde{\rho}_c$, the partial core charge density,[27] equal to the full core density outside the core radius r_c and equal to a smooth function inside the core, where $\rho_c \gg \rho_{ps}$.

The $\Delta\mu_{xc}^{\sigma}$ defined as

$$\Delta\mu_{xc}^{\sigma} = \mu_{xc}^{\sigma}(\rho,\zeta) - \mu_{xc}^{\sigma}(\rho_{ps} + \tilde{\rho}_c,\zeta) \tag{13}$$

vanishes outside the radius at which the pseudocharge density matches the valence charge density. If, as is usually the case, the difference between $\Delta\mu_{xc}^{+}$ and $\Delta\mu_{xc}^{-}$ is small compared to V_{ps} and μ_{xc}^{σ} inside this radius, $\Delta\mu_{xc}$ can be absorbed into V_{ps} resulting in the simpler equations

$$-\nabla^2\phi_i + \left[V_{ps} + \int \frac{2\rho_{ps}(\mathbf{r})}{|\mathbf{r}-\mathbf{r}'|}d\mathbf{r} + \mu_{xc}^{\sigma}(\rho_{ps}+\tilde{\rho}_c,\zeta)\right]\phi_i = \epsilon_i\phi_i, \tag{14}$$

$$i = 1,\ldots,n_v,$$

with ρ_c replaced by $\tilde{\rho}_c$ and still with a single ionic pseudopotential for both spin-up and spin-down electrons.

In the pseudopotential theory, the ionic pseudopotential V_{ps} is assumed to be transferable to different atomic environments and different electronic configurations among the valence electrons. The calculations are then iterated to valence self-consistency. The transferability of the pseudopotential implicitly implies the frozen core approximation. Since the core eigenvalues are determined by a variational procedure, they are correct to second order in $\Delta\rho = \rho - \tilde{\rho}$, where $\tilde{\rho}$ is the "valence self-consistent" charge density. Furthermore, due to the small overlap between the environment induced change in the valence charge density $\Delta\rho_v$ and the smallness of the core region, the second order term has little effect on the valence eigenvalues. Since $\Delta\rho_v$ is mainly localized in the region where ρ_v and ρ_{ps} coincide, the same arguments hold for $\Delta\rho_{ps}$, and the valence eigenvalues are accurately reproduced in a pseudopotential calculation.

It has been shown,[28] that the use of the frozen core approximation in the calculation of total energies is accurate up to second order in $\Delta\rho_c$.

Within this approximation, the total energy is

$$E_{tot} = \sum_{val}\epsilon_i + \sum_{core}\epsilon_i - \frac{1}{2}\int\int \frac{2(\rho_v+\rho_c)(\rho_v'+\rho_c')}{|\mathbf{r}-\mathbf{r}'|}d\mathbf{r}\,d\mathbf{r}' + \sum_{\sigma}\int[\epsilon_{xc}^{\sigma}(\rho_v+\rho_c,\zeta) - \mu_{xc}^{\sigma}(\rho_v+\rho_c,\zeta)] \times\left[\rho_v^{\sigma} + \frac{1}{2}\rho_c\right]d\mathbf{r} + \frac{1}{2}\sum_{\substack{j,j\\ j\neq j}}\frac{2Z_jZ_j}{|\mathbf{R}_j-\mathbf{R}_j|}. \tag{15}$$

Correspondingly, the pseudopotential total energy is defined as

$$E_{ps} = \sum_{val}\epsilon_i - \frac{1}{2}\int\int \frac{2\rho_{ps}\rho_{ps}'}{|\mathbf{r}-\mathbf{r}'|}d\mathbf{r}\,d\mathbf{r}' + \sum_{\sigma}\int\epsilon_{xc}^{\sigma}(\rho_{ps}+\tilde{\rho}_c,\zeta)\left(\rho_{ps}^{\sigma} + \frac{1}{2}\tilde{\rho}_c\right)d\mathbf{r} - \sum_{\sigma}\int\mu_{xc}^{\sigma}(\rho_{ps}+\tilde{\rho}_c,\zeta)\rho_{ps}^{\sigma}d\mathbf{r} + \frac{1}{2}\sum_{\substack{j,j\\ j\neq j}}\frac{2z_jz_j}{|\mathbf{R}_j-\mathbf{R}_j|}, \tag{16}$$

where z_j's are the valence charges and ρ_c and $\tilde{\rho}_c$ denote the superposition of the atomic full and partial cores, respectively ($\frac{1}{2}\rho_c$ in each spin direction).

For calculations of binding energies, vibrational energies, or electronic excitations, one is only interested in total energy differences between various atomic or electronic configurations. These differences are the same whether the frozen core expression (15) or the pseudopotential total energy (16) is used in their evaluation.

This may be seen by examining the configuration-dependent contributions of the various terms in Eqs. (15) and (16), respectively. The first term, the sum over the valence eigenvalues is the same in both expressions. The change in the energies of the frozen core eigenvalues induced by $\Delta\rho_v$ is

$$\sum_{core}\Delta\epsilon_i = \int\int\frac{2\Delta\rho_v}{|\mathbf{r}-\mathbf{r}'|}d\mathbf{r}'\sum_{core}|\psi_i|^2d\mathbf{r} = \int\int\frac{2\Delta\rho_v\rho_c}{|\mathbf{r}-\mathbf{r}'|}d\mathbf{r}\,d\mathbf{r}, \tag{17}$$

which cancels the corresponding first order term in the double-counting correction in Eq. (15). The second order contribution proportional to $\Delta\rho_v\Delta\rho_v$ is the same in both expressions (assuming $\Delta\rho_v = \Delta\rho_{ps}$).

The exchange-correlation contributions to Eq. (15), since $\rho_c \cong \tilde{\rho}_c$ in the region where ρ_{ps} and ρ_c overlap, differ only by a constant. Finally, the dependence of the ion–ion interaction on the atomic position in Eq. (16) is the same as that of the nucleus–nucleus repulsion term in Eq. (15) combined with the "superposition of atomic charges" part of the double-counting correction, provided the non-Coulombic parts of the pseudopotential do not overlap.

The pseudopotentials used in this work have been projected from first-principles all electron atomic calculations following the method of Kerker.[7] The real wave functions were matched at the l-dependent matching radii to a nodeless function $\exp[p(r)]$, where $p(r)$ is a polynomial. Continuity of the pseudo-wave functions and their derivatives and of the resulting l-dependent pseudopotentials and their derivatives were required. The numerical pseudopotentials were fitted to the Gaussian form

$$V_{ps,l}(r) = -\frac{2z}{r}\,\mathrm{erf}(\alpha r) + \sum_i C_i^l\exp(-\beta_i r^2), \tag{18}$$

where l denotes the angular momentum component. The first, "local" term, common to all potentials, is a potential of a spherical Gaussian charge distribution. It has the correct asymptotic ($r\to\infty$) behavior to account for the Coulombic

attraction of the ion. The constant a varied between 1.6 and 2.2 bohr^{-1} depending on the atom. For the short range l-dependent part, 4–6 Gaussians were found sufficient for an accurate fit. The partial core charge density $\tilde{\rho}_c$ was obtained from the atomic core charge density by the procedure of Ref. 27. It was also fitted to Gaussians.

IV. CALCULATIONS

The calculations were carried out using a basis set of atom-centered Gaussians $G_k(\mathbf{r}-\mathbf{R}_j)$ where $\mathbf{R}_j$ denotes the position of jth atom and k denotes the parameter of the Gaussian. The expansion of the wave function ϕ_i is

$$\phi_i = \sum_{j,k} c^i_{jk} G_k(\mathbf{r}-\mathbf{R}_j). \tag{19}$$

Gaussians of s, p, and d symmetry were included in this wave function basis.

With the use of the basis, Eq. (1) becomes a matrix equation

$$\mathbf{H}\mathbf{c}_i = \epsilon_i \mathbf{S}\mathbf{c}_i, \tag{20}$$

where $\mathbf{H}$ and $\mathbf{S}$ are the Hamiltonian and overlap matrices, respectively, and $\mathbf{c}_i$ is a column vector corresponding to the eigenvalue ϵ_i. Since the Hamiltonian is orbital independent, all of the eigenvalues and eigenvectors are generated simultaneously by solving the generalized eigenvalue problem

$$\mathbf{H}\mathbf{C} = \boldsymbol{\epsilon}\mathbf{S}\mathbf{C}, \tag{21}$$

where $\boldsymbol{\epsilon}$ is the eigenvalue vector and $\mathbf{C}$ is the eigenvector matrix, with columns $\mathbf{c}_i$. The resulting eigenvectors are orthonormal.

The use of Gaussian orbitals has the advantage that all the integrals entering the calculation of the matrix elements in Eq. (20) and the total energy in Eq. (16), and not involving the exchange-correlation terms μ^σ_{xc}, and ϵ^σ_{xc}, can be evaluated analytically.[29,30]

Since $\rho = \Sigma|\phi_i|^2$, the straightforward evaluation of the matrix elements of the electron–electron repulsion potential would lead to four-center integrals and the well-known N^4 dependence of the computational effort on the number of basis functions N. This dependence can be reduced to N^3 by fitting the charge density to a set of single center Gaussians[9]:

$$\rho(\mathbf{r}) \cong \bar{\rho}(\mathbf{r}) = \sum_{k,j} d_{kj} G^c_k(\mathbf{r}-\mathbf{R}_j), \tag{22}$$

where the superscript c denotes charge fitting basis. We have used s, p and d Gaussians in this basis.

A least-squares fit which minimizes the error in the classical electron–electron repulsion energy and is constrained by the condition $\int \rho d\mathbf{r} = N_v$, where N_v represents the total number of valence electrons, results in the following expresion for $\mathbf{d}$ (Ref. 11):

$$\mathbf{d} = \mathbf{D}^{-1}(\mathbf{t} + L\mathbf{n}), \tag{23}$$

where the lagrange multiplier L is given by

$$L = (N_v - \mathbf{n}\cdot\mathbf{D}^{-1}\cdot\mathbf{t})/(\mathbf{n}\cdot\mathbf{D}^{-1}\cdot\mathbf{n}) \tag{24}$$

and

$$n_{kj} = \int G^c_k(\mathbf{r}-\mathbf{R}_j)d\mathbf{r}, \tag{25}$$

$$t_{kj} = \iint \frac{G^c_k(\mathbf{r}-\mathbf{R}_j)\rho(\mathbf{r}')}{|\mathbf{r}-\mathbf{r}'|}\,d\mathbf{r}\,d\mathbf{r}', \tag{26}$$

$$D_{kj,k'j'} = \iint \frac{G^c_k(\mathbf{r}-\mathbf{R}_j)G^c_{k'}(\mathbf{r}'-\mathbf{R}_{j'})}{|\mathbf{r}-\mathbf{r}'|}\,d\mathbf{r}\,d\mathbf{r}'. \tag{27}$$

All the above integrals are calculated analytically.

The only three-center Coulomb integrals entering the calculations are in Eq. (26), since the same integrals appear in the calculation of the matrix elements of the fitted Coulomb potential

$$\bar{V}_e(r) = \int \frac{2\bar{\rho}(\mathbf{r}')}{|\mathbf{r}-\mathbf{r}'|}\,d\mathbf{r}'. \tag{28}$$

The exchange-correlation potential μ^σ_{xc} and the energy density ϵ^σ_{xc} must be evaluated numerically. Both were fitted to Gaussians in order to allow for analytical evaluation of the matrix elements in Eq. (19) and the integrals in Eq. (16). Atom-centered s, p, and d functions were used. For this fitting, we have used a least-squares procedure similar to that in Ref. 11. Letting g represent μ^σ_{xc} or ϵ^σ_{xc} and defining

$$n_{kj} = \sum_i w_i G^e_k(\mathbf{r}_i - \mathbf{R}_j), \tag{29}$$

$$t_{kj} = \sum_i w_i G^e_k(\mathbf{r}_i - \mathbf{R}_j) g[\,\rho_t(\mathbf{r}_i)], \tag{30}$$

and

$$D_{kj,k'j'} = \sum_i w_i G^e_k(\mathbf{r}_i - \mathbf{R}_j) G^e_{k'}(\mathbf{r}_i - \mathbf{R}_{j'}) \tag{31}$$

with the constraint

$$\bar{g} = \sum_i w_i g[\,\rho_t(\mathbf{r}_i)]\rho_t(\mathbf{r}_i), \tag{32}$$

where the summation is over the mesh points $\mathbf{r}_i$ with weights w_i, and the fitting coefficients are given by Eq. (23) with N_v replaced by $\bar{g}$. The superscript e denotes the exchange fitting basis. The charge ρ_t in Eqs. (29)–(31) is the sum of the pseudocharge density and the partial core charge density. The constraint (32) imitates the integral entering the evaluation of the total energy (16). In our applications the Lagrange multiplier (24) turned out small showing that this constraint was not important.

The numerical points for evaluating the exchange around each atom were generated from a radial mesh rotated along 24 angular directions.[31] This angular mesh integrates exactly spherical harmonics up to sixth order, which is necessary because of the presence of d orbitals in both the wave function and the charge fitting basis. Since both the pseudocharge density and the partial core charge density are nodeless, we have used a linear radial mesh.

We will now turn to the evaulation of the total energies. Although the pseudopotential total energies are much smaller than the all-electron total energies, they can still reach several hundred Rydbergs for large molecules. Since binding energies are typically of the order of a few eV per atom, a careful evaluation of all terms entering Eq. (16) is necessary.

Let us define ρ_{in} and ρ_{out} as the input and output charge densities in the self-consistent cycle, with $\bar{\rho}_{\text{in}}$ and $\bar{\rho}_{\text{out}}$ denoting the corresponding fitted quantities. The difference

between ρ_{in} and ρ_{out} vanishes during iterations to self-consistency, but the distinction between these two quantities in the evaluation of the total energy helps to provide an early estimate of the binding energy.

If the fitted Coulomb potential [Eq. (28)] is used in Eq. (14), multiplying Eq. (14) by ϕ_i, summing over all occupied orbitals and integrating over r gives

$$\sum_i^{occ}\epsilon_i = T(\rho_{out}) + \int\int \frac{2\rho_{out}\bar{\rho}'_{in}}{|\mathbf{r}-\mathbf{r}'|}\,d\mathbf{r}\,d\mathbf{r}' + \int\left[\sum_j V_j(r-R_j)\right]\rho_{out}\,d\mathbf{r} + \sum_\sigma\int\mu^\sigma_{xc}(\rho_{in},\zeta)\rho^\sigma_{out}\,d\mathbf{r}. \quad (33)$$

Thus, the total pseudopotential energy (16), as a function of ρ_{out}, is

$$E_{ps} = \sum_i^{occ}\epsilon_i + \frac{1}{2}\int\int\frac{2[\,\rho_{out}\rho'_{out} - 2\rho_{out}\bar{\rho}'_{in}\,]}{|\mathbf{r}-\mathbf{r}'|}\,d\mathbf{r}\,d\mathbf{r}' + \sum_\sigma\int\epsilon^\sigma_{xc}(\rho_{out}+\tilde{\rho}_c,\zeta)\left[\rho^\sigma_{out}+\frac{1}{2}\tilde{\rho}_c\right]d\mathbf{r} - \sum_\sigma\int\mu^\sigma_{xc}(\rho_{in}+\tilde{\rho}_c,\zeta)\rho^\sigma_{out}\,d\mathbf{r} + \frac{1}{2}\sum_{\substack{j,j'\\ j\neq j'}}\frac{2z_j z_{j'}}{|\mathbf{R}_j-\mathbf{R}_{j'}|}. \quad (34)$$

The second term in Eq. (34) can be approximated to second order in $\Delta\rho = \rho_{out} - \bar{\rho}_{in}$ by the negative of

$$\bar{V}_{ee} = \frac{1}{2}\int\int\frac{2\bar{\rho}_{in}\bar{\rho}'_{in}}{|\mathbf{r}-\mathbf{r}'|}\,d\mathbf{r}\,d\mathbf{r}'. \quad (35)$$

It is convenient, however, to monitor the first order correction to $\bar{V}_{ee}$ in order to ensure the accuracy of the charge fitting procedure. This correction is given by

$$\Delta = \int\int\frac{2\Delta\rho\bar{\rho}'_{in}}{|\mathbf{r}-\mathbf{r}'|}\,d\mathbf{r}\,d\mathbf{r}' = \int\int\frac{2\rho_{out}\bar{\rho}'_{in} - 2\bar{\rho}_{in}\bar{\rho}'_{in}}{|\mathbf{r}-\mathbf{r}'|}\,d\mathbf{r}\,d\mathbf{r}' = 2(\mathbf{t}\cdot\mathbf{d} - \bar{V}_{ee}), \quad (36)$$

where $\mathbf{t}$ and $\mathbf{d}$ were defined in Eqs. (26) and (23), respectively.

TABLE I. Gaussian decay constants used in the O_2 calculation for the orbital, charge, and exchange basis sets [a.u.]. The $r^2 s$ orbital denotes the $r^2\exp(-\alpha r^2)$ orbital.

Orbital basis	Charge basis	Exchange basis
0.14 s,r^2s,p,d	0.2 s	0.03 s
0.35 s,r^2s,p,d	0.6 s	0.1 s
0.7 s,r^2s,p,d	1.2 s,r^2s,p,d	0.2 s
1.25 s,r^2s,p,d	2.5 s,r^2s,p,d	0.5 s,r^2s,p,d
2.5 s,r^2s,p,d	5.0 s,r^2s,p,d	0.75 s,r^2s,p,d
6.5 s,r^2s,p,d	11.5 s,r^2s,p,d	1.0 s,r^2s,p,d
12.5 s,r^2s,p,d	25.0 s	1.5 s
		2.3 s
		3.3 s
		5.0 s

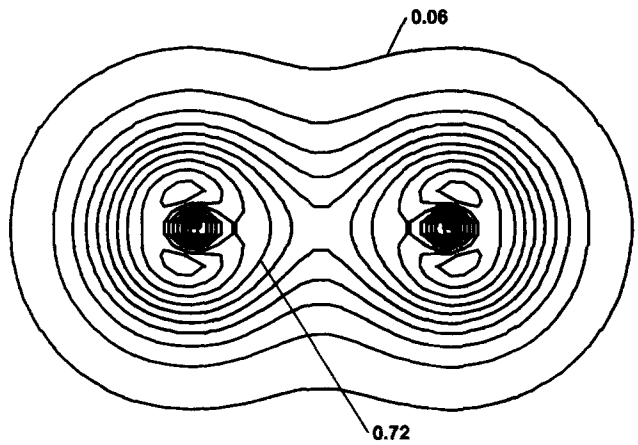

FIG. 1. Contour map of the total pseudocharge density for the O_2 molecule at the experimental equilibrium distance. Linear contour spacing is used and the units are electrons/bohr^3.

V. TEST RESULTS: O_2

We have chosen to test our method on the O_2 molecule, since several all-electron calculations have been carried out for this system.[11–17] In order to compare with previous work, we use the X_α exchange with $\alpha = 0.7$.

The oxygen pseudopotential was generated from the atomic configuration $2s^2 2p^3 3d^1$ with the matching radii $r_{core} = 0.3$, $r_s = 0.68$, and $r_p = r_d = 0.4$ a.u., respectively.[32]

Seven Gaussian decay constants were used for the orbital basis and seven and ten decays were employed in the charge and exchange basis sets, respectively (see Table I). With this basis, the first order correction to the total energy of the molecule (included in the calculations) was below 0.05 Ry for all distances studied.

In Fig. 1 we show the valence pseudocharge density for the molecule. Outside of the matching radii, it agrees very well with the all-electron valence charge distribution reported in Ref. 14. In Table II we compare the nonspin polarized eigenvalues with the results of various all-electron calculations. Finally, in Table III we list the results of spin-polarized total energy calculations in $D_{\infty h}$ symmetry. The eigenvalues, the equilibrium distance, the binding energy, and the vibrational frequency agree very well with the all-electron results.

TABLE II. Comparison of the non-spin-polarized eigenvalues for the O_2 molecule at $r_e = 2.28$ bohr as obtained by the present pseudopotential calculations and various all-electron methods (eV).

Orbital	Present	DV-SCM[a]	FLAPW[b]	DV-LCAO[c]
$2\sigma_g$	−31.72	−31.76	−31.43	−31.69
$1\sigma_u$	−18.75	−18.76	−18.76	−18.59
$3\sigma_g$	−12.50	−12.53	−12.58	−12.39
$1\pi_u$	−12.09	−12.18	−11.74	−12.04
$1\pi_g$	−5.09	−5.21	−4.80	−5.02

[a] Reference 13.
[b] Reference 14.
[c] Reference 15.

TABLE III. Comparison of the calculated equilibrium properties for the O_2 molecule by the present method and various all-electron methods.

	Equilibrium distance (bohr)	Binding energy (eV)	Vibrational frequency (cm^{-1})
Present	2.24	6.7	1575
Gaussian[a]	2.28	7.01	1610
Numerical[b]	2.26	7.1	1620
DVM[c]	2.36	6.6	1570
Experiment	2.28	5.2	1580

[a] Reference 11.
[b] Reference 16.
[c] Reference 17.

We conclude that the present pseudopotential method for localized systems (molecules) is quantitatively as accurate as the all-electron techniques. Similar conclusions have previously been reached for extended systems (solids).[33]

VI. THE ELECTRONIC STRUCTURE OF $Mo_2O_2S_2(S_2)_2^{2-}$

The $Mo_2O_2S_2(S_2)_2^{2-}$ system was first synthesized in 1978 by heating $MoO_2S_2^{2-}$ (Ref. 18). The atomic positions have been subsequently determined from the crystal structure of $[N(CH_3)_4]_2[Mo_2O_2S_2(S_2)_2^{2-}]$ (Ref. 34). The $Mo_2O_2S_2(S_2)_2^{2-}$ ion was found to have approximately C_{2v} symmetry. Since deviations from this symmetry were small and might have been induced by crystal packing, we have used coordinates averaged to full C_{2v} symmetry in the calculations. A perspective drawing of the anion is shown in Fig. 2 and the coordinates are given in Table IV. The S_2 interatomic distance is 2.06 Å compared to 1.89 Å in free S_2.

The calculations have been caried out using four Gaussian decays per atom. Table V lists the decay constants for the orbital basis and the charge and exchange fitting basis sets.

$Mo_2O_2S_2(S_2)_2$ carries a 2^- charge and exists only in solution or in an ionic crystal, where the negative charge is screened by the surrounding medium. We have simulated this effect by occupying the lowest 31 orbitals by two electrons (this corresponds to the 2 — state of the molecule) and scaling the resulting electron–electron repulsion potential by 60/62 (see Ref. 35). The iterations were started with the superposition of atomic charges. The charge was then allowed to relax self-consistently.

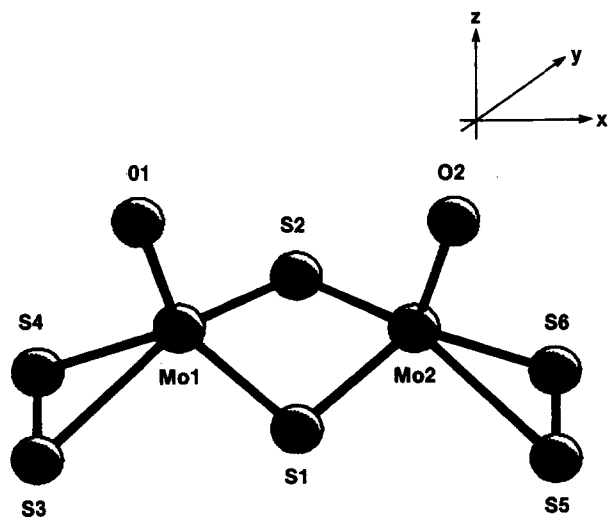

FIG. 2. A perspective view of the $Mo_2O_2S_2(S_2)_2^{2-}$. The insert defines the direction of the coordinate axes as used in the text.

TABLE IV. Atomic coordinates of the $Mo_2O_2S_2(S_2)_2^{2-}$ anion used in the calculation (in Å).

Atom	x	y	z
Mo1	−1.41	0	0
Mo2	1.41	0	0
S1	0	−1.8	−0.37
S2	0	1.8	−0.37
S3	−3.11	−1.03	−1.33
S4	−3.11	1.03	−1.33
S5	3.11	−1.03	−1.33
S6	3.11	1.03	−1.33
O1	−1.89	0	1.61
O2	1.89	0	1.61

In Fig. 3 we show the valence levels of $Mo_2O_2S_2(S_2)_2^{2-}$ (apart from the oxygen and sulfur atoms' s levels) and the Mulliken atomic populations for each level. The figure is divided into Mo, S, S_2, and O panels, in which the populations for each group of atoms are displayed. The S panel represents the bridging sulfur atoms while S_2 denotes the diatomics. For each energy level, the length of the line in each panel is proportional to the Mulliken population for this group of atoms, with the full width of the panel corresponding to 100%. With help of this figure, we will now proceed to describe the molecular orbitals of the system. As is evident from the figure, most of the molecular orbitals are delocalized to some extent and have amplitude on several atoms. This residual interaction between distant atoms results in small splittings among orbitals with similar primary bonding patterns. In the description below, we will only show one contour plot for each primary bonding pattern.

TABLE V. Gaussian decay constants used in the $Mo_2O_2S_2(S_2)_2^{2-}$ calculation for the orbital, charge, and exchange basis sets (in $a.u^{-2}$). Real (Hermite) spherical harmonics were used.

Orbital basis	Charge basis	Exchange basis
Mo		
0.04 s,r^2s,p,d	0.15 s,r^2s,p,d	0.025 s
0.14 s,r^2s,p,d	0.4 r^2s,d	0.085 s
0.45 s,r^2s,p,d	0.9 r^2s,d	0.33 s,r^2s,p,d
1.33 s,r^2s,p,d	1.4 s,r^2s,p,d	1.25 s,r^2s,p,d
	3.0 s,r^2s,p,d	
S		
0.085 s,p	0.2 s	0.065 s
0.25 s,p	0.4 s	0.13 s
0.8 s,r^2s,p,d	0.8 s,r^2s,p,d	0.26 s,r^2s,p,d
1.17 s,p	1.3 s	0.43 s
	2.5 s	0.83 s
O		
0.14 s,p	0.2 s	0.1 s
0.45 s,p	0.6 s	0.33 s,r^2s,p,d
1.4 s,r^2s,p,d	1.7 s,r^2s,p,d	0.83 s,r^2s,p,d
5.5 s,p	3.5 s	1.33 s
	10.5 s	2.33 s
		3.33 s

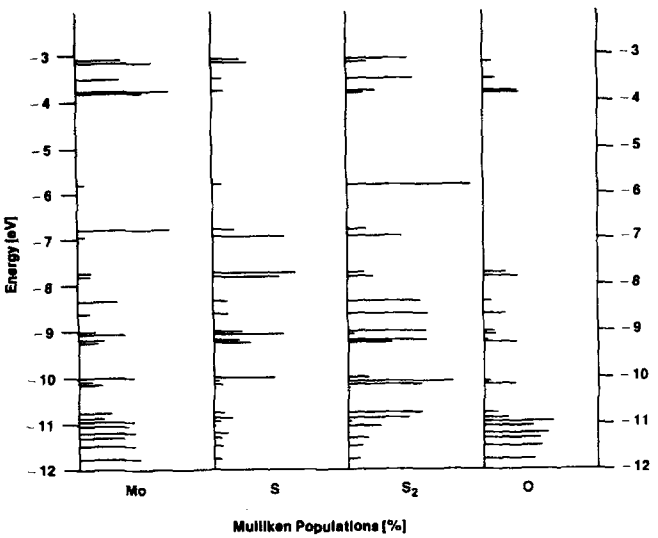

FIG. 3. The energy level diagram for $Mo_2O_2S_2(S_2)_2^{2-}$ and Mulliken populations for Mo, the bridging sulfur atoms, the S_2 diatomics, and the oxygen atoms. For each energy level, the length of the line in the panel is proportional to the relative Mulliken population of this group of atoms with the full width corresponding to 100%.

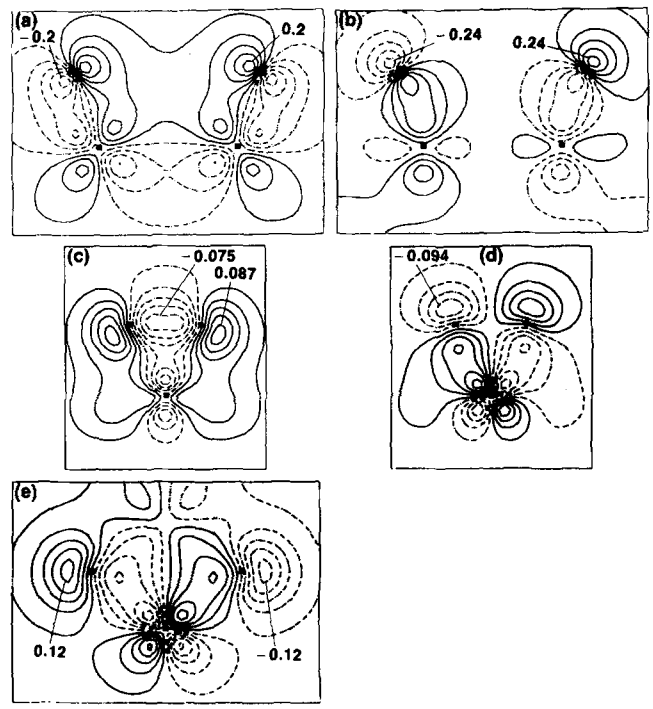

FIG. 4. Contour maps of the occupied low lying valence levels: (a) The Mo–O π bonding state with residual Mo–Mo bonding interaction at -11.74 eV. The plotting plane contains the Mo1, Mo2, O1, and O2 atoms. (b) The Mo–O σ bonding state at -11.27 eV. The plotting plane is the same as in Fig. 4(a). (c) The S_2–Mo bonding state at -10.83 eV. The plotting plane contains the Mo1, S3, and S4 atoms. (d) The S_2–Mo bonding state at -8.31 eV. The same plotting plane as in Fig. 4(c). (e) The $S_{bridging}$–Mo bonding state at -9.97 eV. The plotting plane contains the Mo1, S1, and S2 atoms. Units as in Fig. 1.

The lowest one-electron valence orbitals of this molecule are the oxygen and sulfur s levels with the lowest being the oxygen levels at -25.3 eV, followed by the S_2 $s\sigma$ MOs at -21.0 eV, the bridging sulfur atoms s orbitals at -18.1 eV and finally the S_2 $s\sigma$ antibonding MOs at -16.1 eV.

Among the levels shown in Fig. 3, the Mo–O bonding levels are the lowest. There are six such levels, with significant O and Mo orbital content (see Fig. 3), which indicates that the oxygen atom forms a triple bond to the molybdenum atom in this system. The lowest MO in this group is a π orbital [Fig. 4(a)], with some Mo–Mo bonding interaction. This interaction is responsible for lowering the energy of this orbital below the two σ levels. The σ orbitals [Fig. 4(b)] are followed by the remaining three π orbitals.

We will now turn to the sulfur and molybdenum levels. The energies of sulfur $3p$ (at -7.2 eV) and molybdenum $5s$ and $4d$ (at -4.3 and -4.0 eV) atomic orbitals lie relatively close to each other. For this reason hybrydization and delocalization of the corresponding molecular levels is quite substantial. The molybdenum atomic $5p$ orbitals (at -1.08 eV), on the other hand, do not contribute significantly to the occupied or low-lying unoccupied molecular orbitals.

The S_2 diatomics interact with the molybdenum atom via the $p\sigma$, $p\pi$, and $p\pi^*$ $\|$ orbitals. The five levels with strong S_2–Mo bonding character are at -10.83, -10.71, -9.16, -8.59, and -8.31 eV. The two lowest levels are primarily $p\sigma$ with $p\pi$ admixture and bond to the Mo d (x^2-y^2), d (z^2), and $p(z)$ orbitals [Fig. 4(c)]. The lowest level is also stabilized by residual bonding interaction with the bridging sulfurs atoms. The next two levels are S_2 σ–π levels interacting with Mo d (x^2-y^2) and d (z^2) orbitals. The -8.31 eV level is an S_2 π^* bonding to Mo d (xy) and d (yz) [Fig. 4(d)]. The remaining orbitals with predominantly S_2 character are essentially nonbonding with respect to Mo.

The bridging sulfur atoms form two bonding levels with Mo at -9.97 [Fig. 4(e)] and at -9.02 eV. Both levels involve the Mo d (xy) orbital bonding to the sulfur atoms $p(y)$ and $p(x)$ orbitals, respectively. The bridging sulfur atoms also form a bonding $p\sigma$ orbital with some Mo admixture at -9.18 eV and an antibonding one at -7.8 eV.

We will now describe the levels close to the HOMO-LUMO gap, since these orbitals are most likely to participate in a chemical reaction.

The highest occupied molecular orbitals are the two S_2 $p\pi^*$ [Fig. 5(a)] at -5.8 eV. These orbitals lie in the plane perpendicular to the one defined by the S_2 and Mo atoms. Therefore, they do not interact with Mo. The level below is the Mo–Mo single bond involving the d (x^2-y^2) orbitals [Fig. 5(b)]. The formal oxidation state of Mo is thus Mo(V). This level is at -6.76 eV, almost a volt below the HOMOs. The

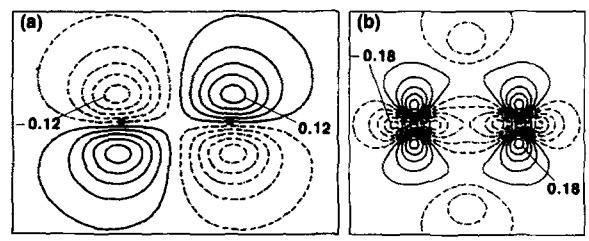

FIG. 5. Contour maps of: (a) The $p\pi^*$ antibonding state of the S_2 at -5.8 eV (HOMO), see the text. The plotting plane contains the S3 and S4 atoms and is perpendicular to the S_2–Mo plane. (b) The Mo–Mo σ bonding state at -6.76 eV. The plotting plane contains the Mo1 and Mo2 atoms and the y axis. Units as in Fig. 1.

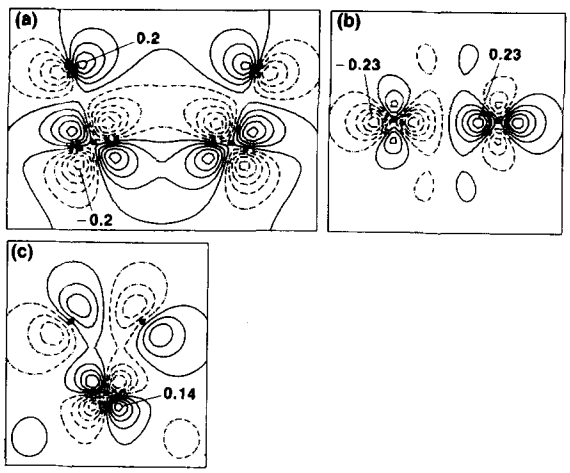

FIG. 6. Contour maps of the low-lying unoccupied orbitals: (a) The Mo–O π^* antibonding state at -3.8 eV. The plotting plane contains the Mo1, Mo2, O1, and O2 atoms. (b) The Mo–Mo antibonding state at -3.77 eV. The plotting plane contains the Mo1 and Mo2 atoms and the y axis. (c) The S_2–Mo antibonding state at -3.5 eV. The plotting plane contains the Mo1, S3, and S4 atoms. Units as in Fig. 1.

Mo–Mo bond may be responsible for the relatively short Mo–Mo distance and the bent shape of the molecule, i.e., for the bridging sulfur atoms not sharing a plane with both metal atoms.

The two levels below the metal–metal bond are the bridging sulfur atoms $p\pi$ (at -7.7 eV) and $p\pi^*$ (at -6.88 eV) orbitals, perpendicular to the Mo–Mo axis. Because the S–S distance is 3.6 Å, the p orbitals perpendicular to the S–S axis interact only weakly and $p\pi$–$p\pi^*$ splitting is small.

The calculated HOMO-LUMO gap in $Mo_2O_2S_2(S_2)_2^{2-}$ is 2 eV indicating a stable molecule. The lowest three unoccupied levels, at -3.8 eV, are two Mo–O π^* antibonding ones, the lower one stabilized slightly by the Mo–Mo interaction [Fig. 6(a)] and the Mo–Mo $d(x^2-y^2)$ antibonding orbital with some O admixture [Fig. 6(b)]. These orbitals are split by 0.03 eV, which is less than the accuracy of the calculation. The next level is the antibonding Mo $d(yz)$–S_2 $p\pi^*$ level at -3.5 eV [Fig. 6(c)]. It is followed by a Mo–Mo $d(x^2-y^2)$ and $d(xz)$ antibonding orbital with significant admixture of the bridging sulfur atoms at -3.15 eV, and another antibonding Mo $d(xy)$–S_2 $p\pi^*$ level at -3.1 eV.

A level structure qualitatively similar to the above was found in other molybdenum–sulfur molecules. These trends in the molybdenum–sulfur bonding patterns will be discussed elsewhere.[36]

VII. SUMMARY AND CONCLUSIONS

We have developed a new method for calculation of the electronic properties of molecules. It is accurate and efficient enough to allow for studies of relatively large systems. It uses first-principles, atom-derived pseudopotentials to describe core-valence interactions and the local density theory of exchange and correlation.

The calculations are carried out by expanding the wave functions, the charge density and the exchange-correlation potential in atom-centered Gaussian orbitals of s, p, and d symmetry. The purely atomic character of the basis helps to maintain uniformity in calculating total energy differences between different geometries and different atomic environments. Since off-center fitting functions are not used, the fitting basis sets are transferable. The effects of nonspherical (non-muffin tin) potentials are included, retaining the original advantage of Gaussian expansion methods[9,11] over the scattered wave X_α procedure.[10]

The method has been tested on the O_2 molecule, for which several all-electron calculations are available in the literature, and found to give results in very good agreement with previous all-electron calculations. In a separate study,[1] this method was also found to reproduce well bonding and dissociation properties of the antiferromagnetically coupled, multiply bonded Mo_2 and Cr_2 systems.

As a first application of the method to a larger system, we have investigated the electronic structure of $Mo_2O_2S_2(S_2)_2^{2-}$. Our results confirm the assignment of the molybdenum atoms oxidation states as Mo(V) by previous workers[18] and the existence of Mo–Mo single bond. The HOMOs, however, turn out to be the S_2 π^* orbitals perpendicular to the Mo-S_2 bonding plane, the Mo–Mo bond being lower by almost 1 eV. We obtain a HOMO-LUMO gap of 2 eV. The LUMOs, which can act as electron acceptors during a reaction process, are the relatively closely spaced π^* antibonding Mo–O, Mo–Mo, and Mo–S_2 orbitals.

The calculations also show that the oxygen atoms form triple bonds to the molybdenums atoms. Since the molybdenum atoms are in the d^1 configuration, the Mo-S and Mo-S_2 bonding interactions are weaker than previously assigned.

ACKNOWLEDGMENTS

It is a pleasure to thank T. H. Upton, E. I. Stiefel, T. Halbert, and W. Pan for valuable discussions.

[1] J. Bernholc and N. A. W. Holzwarth, Phys. Rev. Lett. **50**, 1451 (1983).
[2] J. C. Slater, in *Advances in Quantum Chemistry*, edited by P. O. Loewdin (Academic, New York, 1972), Vol. 6, p. 1.
[3] Since the electron gas contribution corresponds to $\alpha = 2/3$ (Ref. 4), the use of a different from 2/3 may be viewed as an empirical correlation correction.
[4] P. Hohenberg and W. Kohn, Phys. Rev. B **136**, 864 (1964); W. Kohn and L. J. Sham, Phys. Rev. A **140**, 1133 (1965).
[5] L. Hedin and B. I. Lundqvist, J. Phys. C **4**, 2064 (1971).
[6] D. R. Hamann, M. Schluter, and C. Chiang, Phys. Rev. Lett. **43**, 1494 (1979).
[7] G. Kerker, J. Phys. C **13**, L189 (1980).
[8] L. Kleinman, Phys. Rev. B **21**, 2630 (1980).
[9] H. Sambe and R. H. Felton, J. Chem. Phys. **61**, 3862 (1974); **62**, 1122 (1975).
[10] J. C. Slater and K. H. Johnson, Phys. Rev. B **5**, 844 (1972).
[11] B. I. Dunlap, J. W. D. Connolly, and J. R. Sabin, J. Chem. Phys. **71**, 3396 (1979).
[12] B. I. Dunlap, J. W. D. Connolly, and J. R. Sabin, J. Chem. Phys. **71**, 4993 (1979).
[13] B. Delley and D. E. Ellis, J. Chem. Phys. **76**, 1949 (1982).
[14] E. Wimmer, H. Krakauer, M. Weinert, and A. J. Freeman, Phys. Rev. B **24**, 864 (1981).
[15] E. J. Baerends and D. Post, as reported in Ref. 13.
[16] A. D. Becke, J. Chem. Phys. **76**, 6032 (1982).
[17] E. J. Baerends and P. Ros, Int. J. Quantum Chem. Symp. **12**, 169 (1978).
[18] A. Müller, W. Rittner, A. Neumann, and R. C. Sharma, Z. Anorg. Allg. Chem. **472**, 69 (1981).
[19] (a) E. I. Stiefel, in *Molybdenum and Molybdenum-Containing Enzymes*, edited by M. P. Coughlan (Pergamon, New York, 1981); (b) E. I. Stiefel,

Proceeding of the Climax Fourth International Conference on the Chemistry and Uses of Molybdenum, edited by H. F. Barry and P. C. H. Mitchell (Climax Molybdenum, Ann Arbor, MI, 1982).
[20]U. von Barth and L. Hedin, J. Phys. C **5**, 1629 (1972).
[21]O. Gunnarson and B. I. Lundqvist, Phys. Rev. B **13**, 4274 (1976).
[22]S. H. Vosko, L. Wilk, and M. Nusair, Can. J. Phys. **58**, 1200 (1980); L. Wilk and S. H. Vosko, J. Phys. C. **15**, 2139 (1982).
[23]J. Perdew and A. Zunger, Phys. Rev. B **23**, 5048 (1981).
[24]D. M. Ceperley and B. J. Alder, Phys. Rev. Lett. **45**, 566 (1980).
[25]L. R. Kahn and W. A. Goddard III, J. Chem. Phys. **56**, 2685 (1972); C. F Melius and W. A. Goddard III, Phys. Rev. A **10**, 1528 (1974); A. K. Rappe, T. A. Smedley, and W. A. Goddard III, J. Phys. Chem. **85**, 1662 (1981).
[26]P. A. Christiansen, Y. S Lee, and K. S. Pitzer, J. Chem. Phys. **71**, 4445 (1979); L. R. Kahn (unpublished).
[27]S. G. Louie, S. Froyen, and M. L. Cohen, Phys. Rev. B **26**, 1738 (1982).
[28]U. von Barth and C. D. Gelatt, Phys. Rev. **21**, 2222 (1980).
[29]See I. Shavitt, Meth. Comp. Phys. **2**, 1 (1963) for the kinetic energy, overlap, and Coulomb integrals of Gaussian orbitals.
[30]See C. F. Melius, Ph. D thesis, California Institute of Technology, 1972 for the matrix elements of the *l*-dependent pseudopotential.
[31]A. H. Stroud, *Approximate Calculations of Multiple Integrals* (Prentice–Hall, Englewood Cliffs, NJ, 1971), p. 298.
[32]Similar results were obtained using only the *s* and *p* potentials derived from the atomic ground state configuration.
[33]D. R. Hamann, Phys. Rev. Lett. **42**, 662 (1979).
[34]W. Clegg, N. Mohan, A. Müller, A. Neumann, W. Rittner, and G. M. Sheldrick, Inorg. Chem. **19**, 2069 (1980).
[35]This procedure results in an effectively neutral system. Without it, the local density eigenvalues would be positive and the corresponding states would not be normalizable in the usual sense.
[36]J. Bernholc and E. I. Stiefel, Inorg. Chem. (to be published).